Since January 2020 Elsevier has created a COVID-19 resource centre with free information in English and Mandarin on the novel coronavirus COVID-19. The COVID-19 resource centre is hosted on Elsevier Connect, the company's public news and information website.

European Journal of Medicinal Chemistry 206 (2020) 112702

Contents lists available at ScienceDirect

European Journal of Medicinal Chemistry

journal homepage: http://www.elsevier.com/locate/ejmech

Potent inhibitors of SARS-CoV-2 3C-like protease derived from *N*-substituted isatin compounds

Pei Liu [a, 1], Hongbo Liu [a, 1], Qi Sun [a, 1], Hao Liang [a], Chunmei Li [b], Xiaobing Deng [a], Ying Liu [a, b, **], Luhua Lai [a, b, c, *]

[a] BNLMS, State Key Laboratory for Structural Chemistry of Unstable and Stable Species, College of Chemistry and Molecular Engineering, Peking University, Beijing, 100871, China
[b] Center for Quantitative Biology, Peking University, Beijing, 100871, China
[c] Peking-Tsinghua Center for Life Sciences, Peking University, Beijing, 100871, China

ARTICLE INFO

Article history:
Received 15 May 2020
Received in revised form
26 July 2020
Accepted 27 July 2020
Available online 1 August 2020

Keywords:
COVID-19
SARS-CoV-2 3C-like protease
N-substituted isatin compounds
In vitro assay
Structure-activity relationship

ABSTRACT

SARS-CoV-2 3C-like protease is the main protease of SARS-CoV-2 and has been considered as one of the key targets for drug discovery against COVID-19. We identified several *N*-substituted isatin compounds as potent SARS-CoV-2 3C-like protease inhibitors. The three most potent compounds inhibit SARS-CoV-2 3C-like protease with IC_{50}'s of 45 nM, 47 nM and 53 nM, respectively. Our study indicates that *N*-substituted isatin compounds have the potential to be developed as broad-spectrum anti-coronavirus drugs.

1. Introduction

The coronavirus infectious disease 2019 (COVID-19) is a newly emerged infectious disease caused by a novel coronavirus, SARS-CoV-2 [1,2]. COVID-19 has been recognized as a global threat as it rapidly spreads and breaks out in many countries, causing significant health and economic impact. The SARS-CoV-2 is a positive-strand RNA virus that uses a complex set of enzymes to replicate its RNA genome [3,4]. Among these, the 3C-like protease ($3CL^{pro}$), also known as the main protease (M^{pro}), is essential for processing the viral polyproteins that are translated from the viral RNA [5]. The active site of $3CL^{pro}$ contains Cys145 and His41 to constitute a catalytic dyad, in which cysteine functions as the common nucleophile in the proteolytic process [6,7]. The catalytic domain of $3CL^{pro}$ in CoVs is highly conserved [8]. Hence, $3CL^{pro}$ has been considered as an attractive drug target for broad-spectrum anti-coronavirus therapy [4].

A variety of $3CL^{pro}$ inhibitors have been reported in the literature over the past decade [4,9–12]. To date, several potential SARS-CoV-2 $3CL^{pro}$ inhibitors have been reported from compound library screening [8], rational design [8,13,14] and testing of ingredients from traditional Chinese medicine [15,16]. The chemical structures of the experimentally identified SARS-CoV-2 $3CL^{pro}$ inhibitors are diverse, including α-ketoamide analogues [13], peptidomimetics compounds [8,14], baicalein and its derivatives [15,16] and several repurposed approved drugs and drug candidates [8]. However, only a few candidates have high inhibition activity against SARS-CoV-2 $3CL^{pro}$ and no effective therapy has been developed so far.

Previously, we reported a series of *N*-substituted 5-carboxamide-isatin compounds as inhibitors of SARS CoV $3CL^{pro}$ [12]. The best compound showed a sub-micromolar IC_{50} against SARS-CoV $3CL^{pro}$ [12]. Apparently, the isatin scaffold with derivatization may also provide a good starting point for SARS CoV-2 $3CL^{pro}$ inhibitor development, because the two proteases share high sequence identity and the same active site. In order to verify whether isatin compounds can inhibit SARS-CoV-2 $3CL^{pro}$, we

* Corresponding author. BNLMS, State Key Laboratory for Structural Chemistry of Unstable and Stable Species, College of Chemistry and Molecular Engineering, Peking University, Beijing, 100871, China.
** Corresponding author. BNLMS, State Key Laboratory for Structural Chemistry of Unstable and Stable Species, College of Chemistry and Molecular Engineering, Peking University, Beijing, 100871, China.
E-mail addresses: liuying@pku.edu.cn (Y. Liu), lhlai@pku.edu.cn (L. Lai).
[1] These authors contribute equally.

https://doi.org/10.1016/j.ejmech.2020.112702
0223-5234/

selected a series of isatin compounds from an in-house synthetic compound library, synthesized a few new compounds, tested their inhibitory effects against SARS-CoV-2 $3CL^{pro}$, and analyzed their structure-activity relationship (SAR).

2. Results and discussion

2.1. Chemistry

The synthetic route used to prepare the test compounds **1**–**28** is shown in Scheme 1. Compound **26** was resynthesized by a simple and effective synthetic route within three steps. First, 2-((4-carbamoylphenyl)amino)-2-oxoacetimidic acid (**I-26**) was obtained by reaction of 4-aminobenzamide, hydroxylamine hydrochloride, and chloral hydrate. Then, **I-26** was converted into 2,3-dioxoindoline-5-carboxamide (**II-26**) by treatment with concentrated sulfuric acid at 90 °C. Last, **26** was obtained by reaction of 2,3-dioxoindoline-5-carboxamide (**II-26**) with 2-(bromomethyl) naphthalene.

The synthetic route used to prepare compound **29** is shown in Scheme 2, which is different from other compounds. We started from 2-(4-aminophenyl)acetic acid using the general Sandmeyer synthetic route [12,17]. After got 2-(2,3-dioxoindolin-5-yl)acetic acid **(II-29**), additional carboxyl protection to change to methyl 2-(2,3-dioxoindolin-5-yl)acetate (**III-29**) with methyl group, followed by the introduction of naphthyl group at N1 position was subjected to afford methyl 2-(1-(naphthalen-2-ylmethyl)-2,3-dioxoindolin-5-yl)acetate (**IV-29)** and de-protection step to afford 2-(1-(naphthalen-2-ylmethyl)-2,3-dioxoindolin-5-yl)acetic acid (**V-29**). Then through activating the carboxyl group using phosphorus oxychloride, **29** was obtained by reaction of the activated **V-29** and ammonium hydroxide. Compounds **1**–**25** were collected from our synthesized in-house library [12]. Compounds **27**, **28** and **29** are new compounds that have not been reported before. The structures of the newly synthesized compounds **26**, **27**, **28** and **29** and the potent compound **23** were confirmed by ^{1}H NMR, ^{13}C NMR and HRMS.

2.2. Biological evaluation

The inhibition activity was measured following the previously published procedure using a synthetic peptide-pNA as substrate (Table 1) [12,18]. We used Tideglusib as a positive control for the enzyme assay. Our measured IC_{50} value (1.91 μM) is in consistent with the reported one (1.55 μM,Fig. S1). [8] Among all the 29 compounds that we tested, 12 showed inhibition activity over 50% at 50 μM. Hydrophobic groups at the R^1 position are required to insure the inhibitory effect. The carboxamide group at R^2 position (**23**–**28**) is essential for the high inhibition activity. Compounds **26** and **23** inhibit SARS-CoV-2 $3CL^{pro}$ with IC_{50} values of 45 nM (Fig. 1) and 53 nM (Fig. S1), respectively. Further modifications at the 6-position of the naphthalene ring (**27** and **28**) were carried out to study the structure-activity relationship (SAR) of these compounds. Small substituents like 6-bromo in the naphthalene ring can be tolerated with a similar inhibition activity (IC_{50} of 47 nM, Fig. S1) of the parent compound **26**. However, due to space limitation in the enzyme active site, large substituents like 6-phenyl group significantly reduced inhibitory effect (IC_{50} = 24.9 μM, Fig. S1). Substitution to other groups at R^2 position like halogen (**9**), carboxylic acid *N*-hydroxysuccinimide ester (**17**) and ethanamide group (**29**) inactivate or decrease the activity of the compounds. The SARs of these compounds against SARS-CoV-2 $3CL^{pro}$ is similar to that found for SARS-CoV $3CL^{pro}$ [12], further indicating that the substrate binding pocket in $3CL^{pro}$ of CoVs is highly conserved and other classes of reported SARS-CoV or other CoVs $3CL^{pro}$ inhibitors may also be effective against SARS-CoV-2 $3CL^{pro}$.

2.3. Molecular docking study

To examine the potential binding mode of these compounds, we built the complex model structure of **26** and SARS-CoV-2 $3CL^{pro}$ using an induce-fit docking procedure. As shown in Fig. 2, **26** fits snugly into the substrate-binding pocket. The carboxamide at C-5 makes H-bonds with the side-chain carboxyl groups of Asn142 and Glu166, and the oxygens at C-2 and C-3 form H-bonds with the main-chain amino group of Cys145. The naphthyl ring fits into the hydrophobic groove formed by Met49 and Met165 and forms π-π stacking interaction with His41.

Combing the information from structure-activity relationship and docking analysis, we conclude that: (1) The carboxamide group at C-5 is essential for inhibition activity. Even adding one carbon between the carboxamide group and the isatin ring (**29**) was not tolerated. Replacing the carboxamide with carboxylic acid or ester group would destroy the hydrogen bond with Asn142 and bring in charge repulsion, making them unsuitable for binding. (2) The N-1 position of the isatin ring favors hydrophobic aromatic substituents. Aromatic group like naphthalene (**26**) or benzothiophene (**23**) made the molecule more rigid, fit into the pocket well and lead to high inhibition activity. Large substituents in the naphthalene ring significantly reduced activity (**28**).

3. Conclusion

In conclusion, we have tested the inhibition activity of 29 *N*-substituted isatin derivatives against SARS-CoV-2 $3CL^{pro}$. The most potent compound, **26**, demonstrated an IC_{50} of 45 nM against SARS-CoV-2 $3CL^{pro}$, which is among the most potent SARS-CoV-2 $3CL^{pro}$ inhibitors known so far. We found that isatin compounds with a carboxamide substitution at the C-5 position and aromatic substitution at N-1 position are strong inhibitors of SARS-CoV-2 $3CL^{pro}$. As these compounds also inhibit SARS-CoV $3CL^{pro}$, other known SARS-CoV $3CL^{pro}$ inhibitors can be further tested for their inhibition activity against SARS-CoV-2 $3CL^{pro}$. The active compounds have relatively high cytotoxicity that hinder quantitative measurement of their anti-SARS-CoV-2 activity (as shown in Fig. S2). Further optimization to reduce the cytotoxicity and to increase the cellular activity is necessary to develop this series of compounds as broad-spectrum anti-coronavirus drugs.

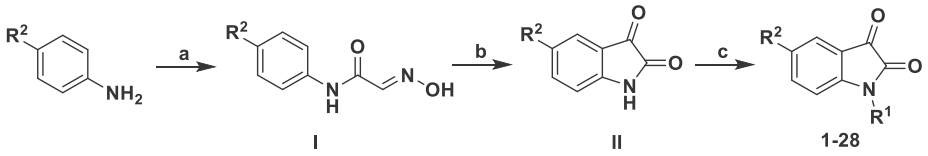

Scheme 1. [a]Reagents and conditions: (a) $Cl_3CCH(OH)_2$, $NH_2OH{\bullet}HCl$, Na_2SO_4, H_2O; (b) H_2SO_4; (c) K_2CO_3, R^1X, acetonitrile.

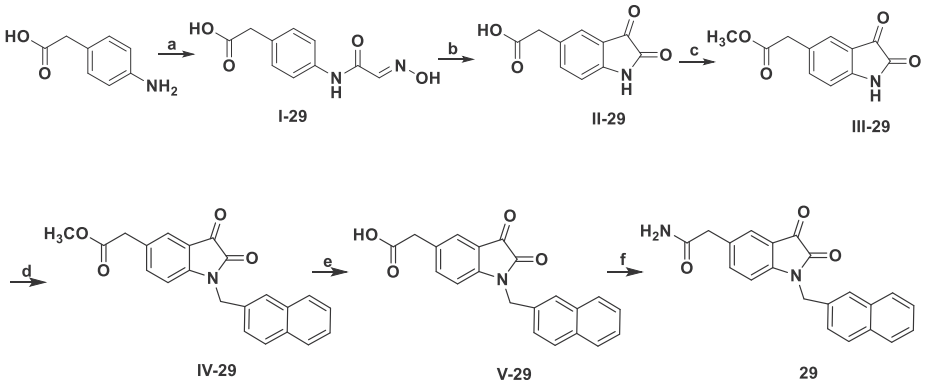

Scheme 2. [a]Reagents and conditions: (a) $Cl_3CCH(OH)_2$, $NH_2OH{\bullet}HCl$, Na_2SO_4, H_2O; (b) H_2SO_4; (c) EDC, dimethylaminopyridine, methanol; (d) K_2CO_3, 2-(Bromomethyl)naphthalene, acetonitrile; (e) NaOH, methanol; (f) i) $POCl_3$; ii) ammonium hydroxide (30%), Et_3N.

4. Experimental section

4.1. Synthesis

Melting points were obtained using an X4 apparatus and are uncorrected. Yields refer to isolated products. ^{1}H NMR (400 MHz or 600 MHz) and ^{13}C NMR (126 MHz or 151 MHz) spectra were measured on a Brucker APX 400 and Bruker-500 spectrometer using TMS as internal standard. The chemical shift values (δ) are reported in ppm relative to tetramethylsilane internal standard. ^{1}H NMR spectra are represented as follows: chemical shift, multiplicity (s = singlet, d = doublet, t = triplet, q = quartet, br = broad, m = multiplet), coupling constant (J values) in Hz and integration. All reactions were monitored by thin layer chromatography (TLC), carried out on silica gel 60 F-254 aluminum sheets using UV, light (254 and 366 nm). The reagents and solvents were available commercially and purified according to conventional methods.

4.1.1. General procedure of the synthesis of compounds ***1*–*28***

4.1.1.1. Synthesis of ***I***.

2-((4-carbamoylphenyl)amino)-2-oxoacetimidic acid (***I*-*26***). Solution A: A 500 mL, three-necked, round-bottomed flask fitted with a condenser and a thermometer was charged with 12.4 g (0.178 mol) of hydroxylamine hydrochloride, 52 g (0.37 mol) of anhydrous sodium sulfate, 14 g (0.085 mol) of chloral hydrate and 230 mL of water. To aid dissolution, the mixture was heated to approximately 70 °C and stirred vigorously with the help of a mechanical stirrer. Solution B: 9.52 g (0.07 mol) of 4-aminobenzamide was added dropwise slowly into a 50-mL round-bottomed flask containing a vigorously stirred mixture of 15 mL of water and 7.5 mL of concentrated sulfuric acid. Solution B was added in one portion to solution A. The mixture was vigorously stirred and heated to reflux. After cooling to room temperature the precipitate was collected by filtration and washed with ice-cold water. 12.31 g (85%) of product was obtained. The crude product is sufficiently pure for the next step.

4.1.1.2. Synthesis of ***II***. 2,3-dioxoindoline-5-carboxamide (***II*-*26***).

A 50-mL, two-necked, round-bottomed flask fitted with a thermometer was charged with 10 mL of concentrated sulfuric acid. After heating and stirring to 70 °C, 10 g (0.048 mol) of **I-26** was added slowly to keep the temperature at 70 °C. The resulting deep red solution was heated to 90 °C for 30 min and then was cooled to room temperature (20 °C) over an ice bath. The mixture was then added rapidly to a vigorously stirred mixture of 100 m L of ice water and 20 mL of ethyl acetate. The organic phase was separated and the aqueous phase was extracted twice with 250 mL of ethyl acetate. The combined red organic phases were dried with sodium sulfate. The solvent was removed under reduced pressure and the crude product was purified by column chromatography. 0.092 g (1%) of an orange powder was obtained.

4.1.1.3. Synthesis of ***1*–*26***.

1-(naphthalen-2-ylmethyl)-2,3-dioxoindoline-5-carboxamide (***26***). A mixture of **II-26** (0.092 g, 0.48 mmol), 2-(Bromomethyl)naphthalene (0.117 g, 0.53 mmol) and K_2CO_3 (0.166 g, 1.20 mmol) in 40 mL of acetonitrile was heating to reflux for 10 h. After the reaction is completed monitored by TLC. The solution was evaporated and purified by column chromatography. 0.079 g (50%) of an orange powder is obtained. m.p.: 290–292 °C. ^{1}H NMR (400 MHz, DMSO-d_6) δ 8.10 (d, J = 1.8 Hz, 1H), 8.07 (dd, J = 8.2, 1.8 Hz, 1H), 8.03 (s, 1H), 8.01 (s, 1H), 7.91 (dd, J = 9.0, 4.8 Hz, 2H), 7.88–7.81 (m, 1H), 7.61–7.54 (m, 1H), 7.54–7.46 (m, 2H), 7.42 (s, 1H), 7.06 (d, J = 8.3 Hz, 1H), 5.11 (s, 2H). ^{13}C NMR (126 MHz, DMSO-d_6) δ 183.08, 166.71, 152.83, 137.71, 133.35, 133.3, 132.82, 129.60, 128.79, 128.06, 126.82, 126.50, 126.18, 125.96, 123.73, 118.16, 111.17, 43.76. HRMS (ESI+) calcd for $C_{20}H_{15}N_2O_3$ $[M + H]^+$: 331.1004, found: 331.1077.

4.1.1.4. *1-(benzo[b]thiophen-2-ylmethyl)-2,3-dioxoindoline-5-carboxamide* (***23***).

An orange powder. m.p.: 210–212 °C. ^{1}H NMR (600 MHz, DMSO-d_6) δ 8.16 (dd, J = 8.3, 1.8 Hz, 1H), 8.11 (d, J = 1.7 Hz, 1H), 8.05 (s, 1H), 7.92 (d, J = 7.9 Hz, 1H), 7.80–7.74 (m, 1H), 7.59 (s, 1H), 7.43 (s, 1H), 7.34 (m, 3H), 5.25 (s, 2H). ^{13}C NMR (151 MHz, DMSO-d_6) δ 182.74, 166.68, 158.83, 152.34, 139.66, 139.53, 139.03, 137.87, 129.83, 125.04, 125.00, 124.05, 123.99, 123.88, 122.98, 118.06, 111.19, 39.51. HRMS (ESI+) calcd for $C_{18}H_{13}N_2O_3S$ $[M + H]^+$: 337.0569, found: 337.0641.

4.1.1.5. *1-((6-Bromonaphthalen-2-yl)methyl)-2,3-dioxoindoline-5-carboxamide* (***27***).

An orange powder. m.p.: 269–271 °C. Yield: 35%. ^{1}H NMR (400 MHz, DMSO-d_6) δ 8.19 (d, J = 1.9 Hz, 1H), 8.11 (d, J = 1.8 Hz, 1H), 8.07 (dd, J = 8.3, 1.9 Hz, 1H), 8.03 (s, 2H), 7.91 (d, J = 8.5 Hz, 1H), 7.82 (d, J = 8.8 Hz, 1H), 7.62 (dd, J = 8.9, 1.9 Hz, 2H), 7.40 (s, 1H), 7.05 (d, J = 8.3 Hz, 1H), 5.10 (s, 2H). ^{13}C NMR (101 MHz, DMSO-d_6) δ 183.02, 166.71, 159.37, 152.75, 137.70, 134.12, 133.99, 131.86, 130.32, 129.95, 129.79, 129.60, 128.03, 127.18, 126.13, 123.74, 119.62, 118.20, 111.11, 43.65. HRMS (ESI+) calcd for $C_{20}H_{14}BrN_2O_3$ $[M + H]^+$: 409.0110, found: 409.0182.

4.1.1.6. *2,3-Dioxo-1-((6-phenylnaphthalen-2-yl)methyl)indoline-5-carboxamide* (***28***).

An orange powder. m.p.: 263–265 °C. Yield: 12%. ^{1}H NMR (400 MHz, DMSO-d_6) δ 8.21 (d, J = 1.8 Hz, 1H), 8.11 (d, J = 1.9 Hz, 1H), 8.08 (dd, J = 8.2, 1.9 Hz, 1H), 8.05–7.92 (m, 4H), 7.83 (m, 3H), 7.60 (dd, J = 8.5, 1.8 Hz, 1H), 7.51 (t, J = 7.7 Hz, 2H),

Table 1
Inhibition activities of isatin derivatives against SARS-CoV-2 $3CL^{pro}$.

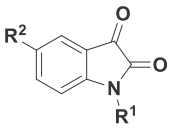

Compds	R^1	R^2	IC_{50} or percentage (%) of inhibition at 50 μM[b]
Tideglusib[a]			1.91 ± 0.16
1	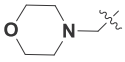	H	-[c]
2	$-CH_2OH$	H	–
3	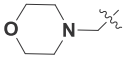	F	–
4	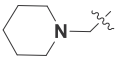	F	–
5	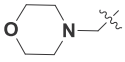	Cl	–
6	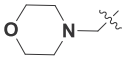	NO_2	–
7	CH_3	I	25% at 50 μM
8	$CH_3CH_2CH_2$	I	51% at 50 μM
9	n-C_4H_9	I	41.8 ± 8.0
10	CH_3	CO_2CH_3	53% at 50 μM
11	$CH_3CH_2CH_2$	CO_2CH_3	53% at 50 μM
12	n-C_4H_9	CO_2CH_3	42% at 50 μM
13	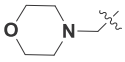	CO_2CH_3	32% at 50 μM
14	$PhCH_2$	CO_2CH_3	45% at 50 μM
15	CH_3	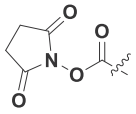	45% at 50 μM
16	n-C_4H_9	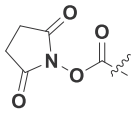	47% at 50 μM
17	$PhCH_2$	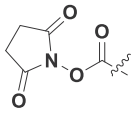	15.5 ± 1.2
18	CH_3	CO_2H	–
19	$CH_3CH_2CH_2$	CO_2H	–
20	n-C_4H_9	CO_2H	–
21	$PhCH_2$	CO_2H	–
22	β-$C_{10}H_7CH_2$	CO_2H	32% at 50 μM
23	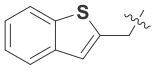	$CONH_2$	0.053 ± 0.010
24	$CH_3CH_2CH_2$	$CONH_2$	10.2 ± 1.0
25	n-C_4H_9	$CONH_2$	17.8 ± 0.7
26	β-$C_{10}H_7CH_2$	$CONH_2$	0.045 ± 0.007
27	β-(6-Br)-$C_{10}H_7CH_2$	$CONH_2$	0.047 ± 0.007
28	β-(6-Ph)-$C_{10}H_7CH_2$	$CONH_2$	24.9 ± 4.6
29	β-$C_{10}H_7CH_2$	CH_2CONH_2	39.2 ± 10.5

[a] Tideglusib was used as positive control. The reported IC50 was 1.55 μM [8], which is in consistent with the value measured in the current study.
[b] Dose-response curves of compounds **Tideglusib**, **9**, **17**, **23**, **24**, **25**, **27**, **28** and **29** are shown in Fig. S1.
[c] Inhibition less than 25% at 50 μM.

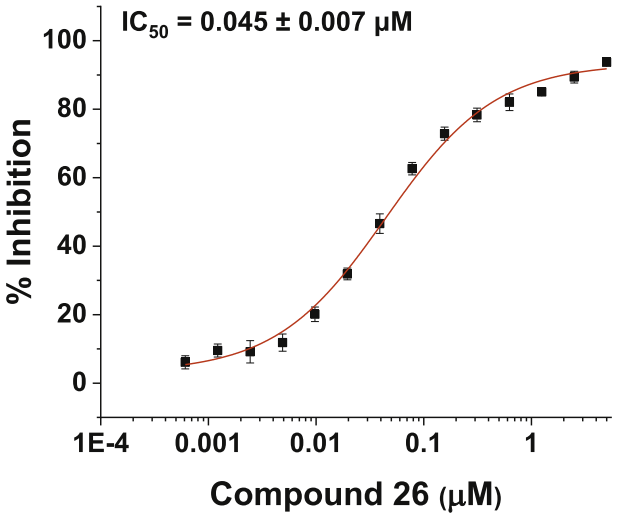

Fig. 1. Dose-response curve of **26** against SARS-CoV-2 3CL^{pro}.

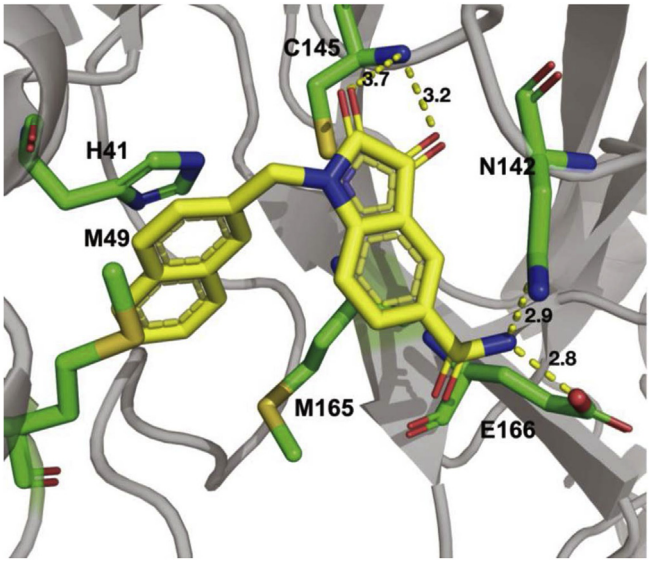

Fig. 2. The complex structure of compound **26** and SARS-CoV-2 3CL^{pro} from docking study. The protein was shown in ribbons, and the compound **26** (yellow) and interacting residues in stick. (For interpretation of the references to color in this figure legend, the reader is referred to the Web version of this article.)

7.44–7.35 (m, 2H), 7.07 (d, J = 8.3 Hz, 1H), 5.13 (s, 2H). ^{13}C NMR (101 MHz, DMSO-d_6) δ 166.72, 159.37, 152.83, 140.30, 138.03, 137.71, 133.49, 133.17, 132.58, 129.49, 129.24, 128.78, 128.06, 127.40, 126.43, 125.95, 125.54, 123.74, 118.18, 111.19, 43.78. ^{13}C NMR (101 MHz, DMSO-d_6) δ 183.09, 166.72, 159.37, 152.83, 140.30, 138.03, 137.71, 133.49, 133.17, 132.58, 129.59, 129.49, 129.24, 128.78, 128.06, 127.40, 126.43, 125.95, 125.54, 123.74, 118.18, 111.19, 43.78. HRMS (ESI+) calcd for $C_{26}H_{19}N_2O_3$ $[M + H]^+$: 407.1317, found: 407.1390.

*4.1.2. Synthesis of compound **29***

*4.1.2.1. Methyl 2-(2,3-dioxoindolin-5-yl)acetate (**III-29**).* To a stirred solution of methanol (50 ml) were added 2-(2,3-dioxoindolin-5-yl) acetic acid **II-29** (2g, 9.7 mmol), 1-Ethyl-3-(3-dimethylaminopropyl)carbodiimide hydrochloride (2.22 g, 11.6 mmol) and 4-dimethylaminopyridine (0.061 g, 0.5 mmol) at 25 °C. After stirring for 3h, the reaction was quenched with 20 ml water. The mixture was extracted with EtOAc and the organic layer was washed with brine, dried over Na_2SO_4, filtered, and concentrated. 1.46 g (70%) of product is obtained. The crude product is sufficiently pure for the next step.

*4.1.2.2. Methyl 2-(1-(naphthalen-2-ylmethyl)-2,3-dioxoindolin-5-yl) acetate (**IV-29**).* A mixture of **III-29** (1 g, 4.6 mmol), 2-(Bromomethyl)naphthalene (1.17 g, 5.3 mmol) and K_2CO_3 (1.63 g, 11.8 mmol) in 100 mL of acetonitrile was heating to reflux for 10 h. After the reaction was completed monitored by TLC. The solution was evaporated and purified by column chromatography. 1.062 g (63%) of a red powder is obtained. ^{1}H NMR (400 MHz, DMSO-d_6) δ 7.99 (s, 1H), 7.95–7.80 (m, 3H), 7.58–7.47 (m, 4H), 7.44 (dd, J = 8.0, 1.7 Hz, 1H), 6.94 (d, J = 8.1 Hz, 1H), 5.07 (s, 2H), 3.68 (s, 2H), 3.58 (s, 3H).

*4.1.2.3. 2-(1-(naphthalen-2-ylmethyl)-2,3-dioxoindolin-5-yl)acetic acid (**V-29**).* Methyl ester **IV-29** (1g, 2.78 mmol) was dissolved in 100 ml methanol. NaOH (0.117 g, 2.92 mmol) was added to this solution. The mixture was stirred at 55–60 °C for 1 h. After cooling to the room temperature, 20 ml 3 N HCl was added. The precipitate was collected by filtration and washed with ice-cold water twice. 0.859 g (89%) of an orange power is obtained.

*4.1.2.4. 2-(1-(naphthalen-2-ylmethyl)-2,3-dioxoindolin-5-yl)acetamide (**29**).* To a stirred solution of EtOAc (5 ml) and THF (5 ml) added compound **V-29** (30 mg, 0.08 mmol), $POCl_3$ (110 mg, 0.71 mmol) over an ice bath. The mixture was stirred for additional 30 min. Then the resulting solution was adder to another mixture containing 5 ml acetonitrile, 30% ammonium hydroxide (0.560 g, 10 mmol) and Et_3N (1.01 g, 10 mmol). After the reaction completed, the mixture was extracted with EtOAc and the organic layer was washed with brine, dried over Na_2SO_4, filtered, and concentrated. The residue was purified by silica gel column chromatography to give the **29** (15 mg, 57%) as an orange powder. m.p.: 200–202 °C. ^{1}H NMR (400 MHz, DMSO-d_6) δ 7.98 (s, 1H), 7.96–7.81 (m, 3H), 7.60–7.44 (m, 5H), 7.40 (dd, J = 8.2, 1.9 Hz, 1H), 6.92 (d, J = 8.1 Hz, 2H), 5.07 (s, 2H), 3.34 (s, 2H). ^{13}C NMR (126 MHz, DMSO-d_6) δ 172.94, 149.48, 139.36, 133.50, 133.35, 132.82, 130.85, 128.82, 128.08, 128.04, 126.81, 126.48, 126.22, 125.93, 118.16, 111.32, 43.65, 39.78. HRMS (ESI+) calcd for $C_{21}H_{17}N_2O_3$ $[M + H]^+$: 345.1161, found: 345.1234.

4.2. Molecular docking

The crystal structure of SARS-CoV-2 3CL^{pro} (PDB ID 6LU7) was used for molecular docking [8]. The structures of the protein and **26** were prepared by Protein Preparation Wizard and LigPrep module, respectively. The binding pocket was defined as a 20*20*20 Å^3 cubic box centered to the centroid of Cys145. Flexible docking was conducted using the Induced Fit Docking module in GLIDE. Standard protocol and XP precision were used. Ten conformations were generated and scored by glidescore. The best scored conformation was used for structural analysis. All the above mentioned modules were implemented in Schrödinger version 2015-4 (Schrödinger software suite, L. L. C. New York, NY (2015).)

4.3. Biology

4.3.1. Cloning, expression and purification of SARS-CoV-2 3CL^{pro}

The full-length gene encoding SARS-CoV-2 3CL^{pro} was synthesized for *Escherichia coli* (*E. coli*) expression (Hienzyme Biotech). The expression and purification of SARS-CoV-2 3CL^{pro} were carried out using the reported protocol [15].

4.3.2. Enzyme assay

A colorimetric substrate Thr-Ser-Ala-Val-Leu-Gln-pNA (GL Biochemistry Ltd) and assay buffer (40 mM PBS, 100 mM NaCl, 1 mM EDTA, 0.1% Triton 100, pH 7.3) was used for the inhibition assay. To evaluate the effects of compounds on SARS-CoV-2 3CL protease activity, compounds were first pre-incubated with enzyme samples in the assay buffer for 30 min at room temperature. And then 10 μl of 2 mM substrate was added into the above system to the final concentration of 200 μM to initiate the reaction. Increase in absorbance at 390 nm was recorded for 20 min at an interval of 30s with a kinetics mode program using a plate reader (Synergy, Biotek). IC_{50} values were fitted with Hill1 function.

Declaration of competing interest

The authors declare that they have no conflicts of interest to this work.

Acknowledgements

This work was supported in part by the National Natural Science Foundation of China (21633001,21877003), and the Ministry of Science and Technology of China (2016YFA0502303).

Abbreviations

COVID-19	CoV infectious disease
$3CL^{pro}$	3C-like protease
TLC	thin layer chromatography

Appendix. Supplementary data

Supplementary data associated with this article can be found in the online version, at https://doi.org/10.1016/j.ejmech.2020.112702. These data include MOL files and InChiKeys of the most important compounds described in this article.

References

[1] N. Zhu, D. Zhang, W. Wang, X. Li, B. Yang, J. Song, X. Zhao, B. Huang, W. Shi, R. Lu, P. Niu, F. Zhan, X. Ma, D. Wang, W. Xu, G. Wu, G.F. Gao, W. Tan, I. China Novel Coronavirus, T. Research, A novel coronavirus from patients with pneumonia in China, 2019, N. Engl. J. Med. 382 (2020) 727–733, https://doi.org/10.1056/nejmoa2001017.

[2] P. Zhou, X.L. Yang, X.G. Wang, B. Hu, L. Zhang, W. Zhang, H.R. Si, Y. Zhu, B. Li, C.L. Huang, H.D. Chen, J. Chen, Y. Luo, H. Guo, R.D. Jiang, M.Q. Liu, Y. Chen, X.R. Shen, X. Wang, X.S. Zheng, K. Zhao, Q.J. Chen, F. Deng, L.L. Liu, B. Yan, F.X. Zhan, Y.Y. Wang, G.F. Xiao, Z.L. Shi, A pneumonia outbreak associated with a new coronavirus of probable bat origin, Nature 579 (2020) 270–273, https://doi.org/10.1038/s41586-020-2012-7.

[3] A. Zumla, J.F. Chan, E.I. Azhar, D.S. Hui, K.Y. Yuen, Coronaviruses - drug discovery and therapeutic options, Nat. Rev. Drug Discov. 15 (2016) 327–347, https://doi.org/10.1038/nrd.2015.37.

[4] T. Pillaiyar, M. Manickam, V. Namasivayam, Y. Hayashi, S.H. Jung, An overview of severe acute respiratory syndrome-coronavirus (SARS-CoV) 3CL protease inhibitors: peptidomimetics and small molecule chemotherapy, J. Med. Chem. 59 (2016) 6595–6628, https://doi.org/10.1021/acs.jmedchem.5b01461.

[5] R. Hilgenfeld, From SARS to MERS: crystallographic studies on coronaviral proteases enable antiviral drug design, FEBS J. 281 (2014) 4085–4096, https://doi.org/10.1111/febs.12936.

[6] K. Anand, J. Ziebuhr, P. Wadhwani, J.R. Mesters, R. Hilgenfeld, Coronavirus main proteinase ($3CL^{pro}$) structure: basis for design of anti-SARS drugs, Science 300 (2003) 1763–1767, https://doi.org/10.1126/science.1085658.

[7] Q.S. Du, S.Q. Wang, Y. Zhu, D.Q. Wei, H. Guo, S. Sirois, K.C. Chou, Polyprotein cleavage mechanism of SARS CoV M^{pro} and chemical modification of the octapeptide, Peptides 25 (2004) 1857–1864, https://doi.org/10.1016/j.peptides.2004.06.018.

[8] Z. Jin, X. Du, Y. Xu, Y. Deng, M. Liu, Y. Zhao, B. Zhang, X. Li, L. Zhang, C. Peng, Y. Duan, J. Yu, L. Wang, K. Yang, F. Liu, R. Jiang, X. Yang, T. You, X. Liu, X. Yang, F. Bai, H. Liu, X. Liu, L.W. Guddat, W. Xu, G. Xiao, C. Qin, Z. Shi, H. Jiang, Z. Rao, H. Yang, Structure of M^{pro} from COVID-19 virus and discovery of its inhibitors, Nature 582 (2020) 289–293, https://doi.org/10.1038/s41586-020-2223-y.

[9] H. Konno, T. Onuma, I. Nitanai, M. Wakabayashi, S. Yano, K. Teruya, K. Akaji, Synthesis and evaluation of phenylisoserine derivatives for the SARS-CoV 3CL protease inhibitor, Bioorg. Med. Chem. Lett 27 (2017) 2746–2751, https://doi.org/10.1016/j.bmcl.2017.04.056.

[10] K. Ohnishi, Y. Hattori, K. Kobayashi, K. Akaji, Evaluation of a non-prime site substituent and warheads combined with a decahydroisoquinolin scaffold as a SARS 3CL protease inhibitor, Bioorg. Med. Chem. 27 (2019) 425–435, https://doi.org/10.1016/j.bmc.2018.12.019.

[11] S.I. Yoshizawa, Y. Hattori, K. Kobayashi, K. Akaji, Evaluation of an octahydroisochromene scaffold used as a novel SARS 3CL protease inhibitor, Bioorg. Med. Chem. 28 (2020) 115273, https://doi.org/10.1016/j.bmc.2019.115273.

[12] L. Zhou, Y. Liu, W.L. Zhang, P. Wei, C.K. Huang, J.F. Pei, Y.X. Yuan, L.H. Lai, Isatin compounds as noncovalent SARS coronavirus 3C-like protease inhibitors, J. Med. Chem. 49 (2006) 3440–3443, https://doi.org/10.1021/jm0602357.

[13] L. Zhang, D. Lin, X. Sun, U. Curth, C. Drosten, L. Sauerhering, S. Becker, K. Rox, R. Hilgenfeld, Crystal structure of SARS-CoV-2 main protease provides a basis for design of improved alpha-ketoamide inhibitors, Science 368 (2020) 409–412, https://doi.org/10.1126/science.abb3405.

[14] W. Dai, B. Zhang, H. Su, J. Li, Y. Zhao, X. Xie, Z. Jin, F. Liu, C. Li, Y. Li, F. Bai, H. Wang, X. Cheng, X. Cen, S. Hu, X. Yang, J. Wang, X. Liu, G. Xiao, H. Jiang, Z. Rao, L.-K. Zhang, Y. Xu, H. Yang, H. Liu, Structure-based design of antiviral drug candidates targeting the SARS-CoV-2 main protease, Science (2020) eabb4489, https://doi.org/10.1126/science.abb4489.

[15] H. Liu, F. Ye, Q. Sun, H. Liang, C. Li, R. Lu, B. Huang, W. Tan, L. Lai, Extract and Baicalein Inhibit Replication of SARS-CoV-2 and its 3C-like Protease, bioRxiv, 2020, https://doi.org/10.1101/2020.04.10.035824, 2020.2004.2010.035824.

[16] H. Su, S. Yao, W. Zhao, M. Li, J. Liu, W. Shang, H. Xie, C. Ke, M. Gao, K. Yu, H. Liu, J. Shen, W. Tang, L. Zhang, J. Zuo, H. Jiang, F. Bai, Y. Wu, Y. Ye, Y. Xu, Discovery of Baicalin and Baicalein as Novel, Natural Product Inhibitors of SARS-CoV-2 3CL Protease, bioRxiv, 2020, https://doi.org/10.1101/2020.04.13.038687, 2020.2004.2013.038687.

[17] T. Sandmeyer, Über isonitrosoacetanilide und deren Kondensation zu Isatinen, Helv. Chim. Acta 2 (1919) 234–242, https://doi.org/10.1002/hlca.19190020125.

[18] C. Huang, P. Wei, K. Fan, Y. Liu, L. Lai, 3C-like proteinase from SARS coronavirus catalyzes substrate hydrolysis by a general base mechanism, Biochemistry 43 (2004) 4568–4574, https://doi.org/10.1021/bi036022q.